

CERN-PH-EP-2012-369
18 January 2013

CERN-PH-EP-2012-369
LHWG-Note 2012-01
ALEPH 2012-001 PHYSICS 2012-001
DELPHI 2012-001 PHYS 953
L3 Note 2835
OPAL PR433
December 19, 2012

Search for Charged Higgs bosons: Combined Results Using LEP data

ALEPH, DELPHI, L3 and OPAL Collaborations
The LEP working group for Higgs boson searches¹

Abstract

The four LEP collaborations, ALEPH, DELPHI, L3 and OPAL, have searched for pair-produced charged Higgs bosons in the framework of Two Higgs Doublet Models (2HDMs). The data of the four experiments are statistically combined. The results are interpreted within the 2HDM for Type I and Type II benchmark scenarios. No statistically significant excess has been observed when compared to the Standard Model background prediction, and the combined LEP data exclude large regions of the model parameter space. Charged Higgs bosons with mass below $80 \text{ GeV}/c^2$ (Type II scenario) or $72.5 \text{ GeV}/c^2$ (Type I scenario, for pseudo-scalar masses above $12 \text{ GeV}/c^2$) are excluded at the 95% confidence level.

To be submitted to Eur. Phys. Journal C

¹The authors are listed in Refs.[2,3,5,6,8].

1 Introduction

More than twelve years after the end of data-taking at LEP, it is still useful to add to the LEP legacy the outcome of the searches for a charged Higgs boson. In fact, the charged Higgs boson searches at hadron colliders are restricted to specific decay channels, thus having (yet) some difficulties to provide limits in the charged Higgs boson mass independent of $\tan\beta$ (the ratio of the two Higgs doublet vacuum expectation values).

Since the previous communication by the LEP working group for Higgs boson searches (LEPHWG) on charged Higgs boson searches, in 2001 [1], the LEP experiments have published their final results on these searches and have, in some cases, also added searches for new final states not previously considered. The four LEP collaborations have searched for charged Higgs bosons in the framework of Two Higgs Doublet Models (2HDMs). Based on the final results obtained by ALEPH [2], DELPHI [3,4], L3 [5] and OPAL [6,7], the LEPHWG has performed a statistical combination of the data taken at centre-of-mass energies, \sqrt{s} , from 183 GeV to 209 GeV. The total luminosity used in this combination is 2.6 fb^{-1} .

The existence of a pair of charged Higgs bosons is predicted by several extensions of the Standard Model (SM). In 2HDMs, the charged Higgs couplings to the photon and the Z boson are completely specified in terms of the electric charge and the weak mixing angle, θ_W , and therefore, at tree level, the production cross-section depends only on the charged Higgs boson mass. Higgs bosons couple proportionally to the particle mass and therefore decay preferentially to heavy particles, but the precise branching ratios may vary significantly depending on the model. Two scenarios are considered in this paper. The first one effectively allows the charged Higgs boson to decay to fermions only, which is the case in type II 2HDM [9] for not too small values of m_A (the neutral CP-odd A boson mass) or $\tan\beta$. In this model the isospin $+\frac{1}{2}$ fermion-couplings to the charged Higgs boson are proportional to $1/\tan\beta$, while the isospin $-\frac{1}{2}$ fermion-couplings are proportional to $\tan\beta$. This scenario is treated in Section 2. In the second scenario, type I 2HDM [10], all fermions couple proportionately to $1/\tan\beta$. Consequently, the second scenario effectively allows the charged Higgs boson to also decay into gauge (possibly off-shell) bosons and Higgs bosons (see Section 3).

At LEP, charged Higgs bosons are pair-produced, via s-channel exchange of a Z^0 boson (real or virtual). Electroweak precision measurements set indirect bounds on the mass of the charged Higgs boson regardless of its decay branching ratios. The difference between the measured decay width of the Z^0 (Γ_Z) and the prediction from the SM sets a limit on any non-standard (non SM) contribution to Z^0 decay. The Z^0 decay width has been measured precisely during the first phase of LEP (LEP-1). The final LEP result [11] set the limit $\Gamma_{\text{nonSM}} < 2.9 \text{ MeV}/c^2$ (95% C.L.), which translates to $m_{H^\pm} > 39.6 \text{ GeV}/c^2$ (95% C.L.). Direct searches during the LEP-1 period set a lower bound for the charged Higgs boson mass at $44.1 \text{ GeV}/c^2$ at 95% C.L. for type II 2HDM [12-15]. The combination in this paper is performed for charged Higgs boson masses of $43 \text{ GeV}/c^2$ or larger, since the region below $43 \text{ GeV}/c^2$ has been covered by individual experiments.

For this combination of data, the cross-sections (and branching ratios for type II 2HDM)

are calculated within the HZHA program package [16], and the branching ratios of the charged Higgs boson in type I 2HDM are taken from Ref. [17].

The input from the four experiments [2-7] which is used in the combination procedure is provided on a channel-by-channel basis. The word “channel” designates any subset of the data where a Higgs boson search has been carried out. These subsets may correspond to specific final-state topologies, to data sets collected at different centre-of-mass energies or to the subsets of data collected by different experiments. Table 1 shows a summary of all channels available for this combination. It amounts to 22 channels from ALEPH, 43 from DELPHI, 12 from L3 and 45 from OPAL.

Each experiment generated and simulated the detailed detector response in Monte Carlo event samples for the Higgs signal and the various background processes, at centre-of-mass energies of 183, 189, 192, 196, 200, 202, 204, 206, 208 and 209 GeV to estimate background and signal contributions in the data collected between 1997 and 2000. Particular care has been taken when simulating the four-fermion background, especially from W-pair background, using the most advanced codes available at that time. ALEPH used KORALW [18] as the generator and RACOONWW [19] and YFSWW [20] for the cross-section calculation, while DELPHI used WPHACT [21], L3 YFSWW and OPAL GRC4F [22] and KORALW. Other generators were used for systematic studies. Furthermore, each of the four experiments used different values for the W mass in these background simulations (respectively 80.45, 80.40, 80.356 and 80.33 GeV/ c^2 for ALEPH, DELPHI, L3 and OPAL), while the LEP combined measured value is 80.376 GeV/ c^2 [23], thus introducing an additional source of systematic uncertainty.

Experiment (Ref.)	Final state	\sqrt{s} (GeV)	\mathcal{L} (pb^{-1})	m_{H^\pm} range (GeV/ c^2)
ALEPH [2]	$\text{H}^+\text{H}^- \rightarrow \text{c}\bar{\text{s}}\text{c}\text{s}$	189 - 209	630	45 - 100
	$\text{H}^+\text{H}^- \rightarrow \text{c}\bar{\text{s}}\tau\nu$	189 - 209	630	55 - 100
	$\text{H}^+\text{H}^- \rightarrow \tau\nu\tau\nu$	189 - 209	630	45 - 100
DELPHI [3],[4]	$\text{H}^+\text{H}^- \rightarrow \text{c}\bar{\text{s}}\text{c}\text{s}$	183 - 209	650	40 - 100
	$\text{H}^+\text{H}^- \rightarrow \text{c}\bar{\text{s}}\tau\nu$	183 - 209	625	40 - 100
	$\text{H}^+\text{H}^- \rightarrow \tau\nu\tau\nu$	183 - 209	620	40 - 100
	$\text{H}^+\text{H}^- \rightarrow \text{W}^*\text{A}\tau\nu$	189 - 209	600	40 - 100
	$\text{H}^+\text{H}^- \rightarrow \text{W}^*\text{A}\text{W}^*\text{A}$	189 - 209	600	40 - 100
L3 [5]	$\text{H}^+\text{H}^- \rightarrow \text{c}\bar{\text{s}}\text{c}\text{s}$	183 - 209	685	50 - 100
	$\text{H}^+\text{H}^- \rightarrow \text{c}\bar{\text{s}}\tau\nu$	183 - 209	685	50 - 100
	$\text{H}^+\text{H}^- \rightarrow \tau\nu\tau\nu$	183 - 209	685	50 - 100
OPAL [6],[7]	$\text{H}^+\text{H}^- \rightarrow \text{c}\bar{\text{s}}\text{c}\text{s}$	183 - 209	670	40 - 100
	$\text{H}^+\text{H}^- \rightarrow \text{c}\bar{\text{s}}\tau\nu$	183 - 209	670	40 - 100
	$\text{H}^+\text{H}^- \rightarrow \tau\nu\tau\nu$	183 - 209	680	45 - 100
	$\text{H}^+\text{H}^- \rightarrow \text{W}^*\text{A}\tau\nu$	189 - 209	600	40 - 95
	$\text{H}^+\text{H}^- \rightarrow \text{W}^*\text{A}\text{W}^*\text{A}$	189 - 209	600	40 - 95

Table 1: Overview of the searches for charged Higgs bosons performed by the four LEP experiments, whose results are used in this combination. Where relevant, m_{A} varies from $2m_{\text{b}}$ to m_{H^\pm} .

The statistical procedure adopted for the combination of the data and the precise definitions of the confidence levels CL_b , CL_s , CL_{s+b} by which the search results are expressed, have been described previously [24]. The main sources of systematic uncertainty affecting the signal and background predictions are included, using an extension of the method of Cousins and Highland [25] where the p-values are averaged over a large ensemble of Monte Carlo experiments. The correlations between search channels, LEP collision energies and individual experiments have not been taken into account, but these correlations are estimated to have only small effects, about $500 \text{ MeV}/c^2$, to the final results.

2 Combined searches in the framework of type II 2HDM

In 2HDMs there are five physical Higgs bosons: the CP-even h and H , the CP-odd A and the charged Higgs bosons, H^\pm . The various types of the 2HDMs differ by their couplings to the SM fermions. In type II 2HDM [9], one Higgs doublet couples to up-type fermions and the other to down-type fermions. The Higgs sector of the Minimal Supersymmetric Standard Model (MSSM) is a particular case of such models. In the MSSM, at tree-level, the H^\pm is constrained to be heavier than the W boson and the radiative corrections to the charged Higgs mass are positive, except for very specific parameter choices. Thus, experimentally finding evidence of a charged Higgs boson with mass below the W boson mass would set very strong constraints on the MSSM parameters. However, in the following we will concentrate on the general type II 2HDM without any supersymmetric assumptions. Results on the search for neutral MSSM Higgs bosons can be found in [26].

For the charged Higgs masses accessible at LEP energies, the decays into $\tau^+\nu_\tau$ and $c\bar{s}$ (and their charge conjugates) are expected to dominate. The searches are carried out under the assumption that the two decays $H^+ \rightarrow c\bar{s}$ and $H^+ \rightarrow \tau^+\nu$ exhaust the H^+ decay width, but the relative branching ratio is free. This assumption is valid as long as m_A is larger than $60 \text{ GeV}/c^2$ (MSSM case) or $\tan\beta$ is large. Thus, the searches encompass the following H^+H^- final states: $(c\bar{s})(\bar{c}s)$, $(\tau^+\nu)(\tau^-\bar{\nu})$ and the mixed mode $(c\bar{s})(\tau^-\bar{\nu})$ or $(\bar{c}s)(\tau^+\nu)$. The combined search results are presented as a function of the branching ratio $\text{Br}(H^+ \rightarrow \tau^+\nu)$.

Details of the searches done by the individual experiments can be found in Refs. [2-7]. Two features in these analyses are worth noting: the main background is W pair production, which is partly irreducible, and the reconstructed mass is one of the discriminant variables used in the final hypothesis testing in the two channels where this is relevant (mixed and hadronic channels). The results from the four LEP experiments are summarised in Table 2, together with the 95% C.L. observed and median expected lower limits on the charged Higgs boson mass. The mass limits are quoted separately for $\text{Br}(H^+ \rightarrow \tau^+\nu) = 0, 1$, and independently of the charged Higgs decay.

In a first step, the statistical combination software was run separately on the data provided by the four collaborations and the results (shown in Figure 1) compared to the published results of each. The differences between this check and the published results reflect the differences

Experiment	ALEPH [2]	DELPHI [3]	L3 [5]	OPAL [6]
Total Int. luminosity (pb^{-1})	630	620	685	670
Final states	Number of expected/observed events (*)			
$(c\bar{s})(\bar{c}s)$	2806.0/2742	2179.3/2179	2473.8/2578	1501.4/1471
$(c\bar{s})(\tau^-\bar{\nu})$	289.3/280	1122.8/1129	494.5/470	526.3/569
$(\tau^+\nu)(\tau^-\bar{\nu})$	39.8/45	73.6/66	149.8/147	1103.4/1110
Sum of all channels	3135.1/3067	3375.7/3374	3118.1/3195	3131.1/3150
Mass limits in GeV/c^2				
Expected(median)/ observed limit				
$\text{Br}(\text{H}^+\rightarrow\tau^+\nu)=0$	78.2/80.4	77.7/77.8	76.8/76.6	77.2/76.5
$\text{Br}(\text{H}^+\rightarrow\tau^+\nu)=1$	89.2/87.8	88.9/90.1	84.3/83.7	89.2/91.3
any $\text{Br}(\text{H}^+\rightarrow\tau^+\nu)$	77.1/79.3	76.3/74.4	75.7/76.4	75.6/76.3

Table 2: *Individual search results for the $e^+e^-\rightarrow\text{H}^+\text{H}^-$ fermionic final states. All limits are given at the 95% C.L.. (*) The OPAL selection is mass-dependent; the numbers given here are for $m_{\text{H}^\pm}=80 \text{ GeV}/c^2$.*

between the statistical methods used by the four collaborations. The biggest difference has been found for the expected limit from OPAL at $\text{Br}(\text{H}^+\rightarrow\tau^+\nu)=1$ and amounts to $600 \text{ MeV}/c^2$. This difference is compatible in size with the estimated effect of about $500 \text{ MeV}/c^2$ of not taking into account the correlations between systematic uncertainties. All mass limits have thus been rounded down to the nearest half a GeV/c^2 .

Combining the results from the four experiments, a scan in the branching ratio $\text{Br}(\text{H}^+\rightarrow\tau^+\nu)$ versus charged Higgs boson mass plane has been performed, and the limit-setting procedure was repeated for each scan point. This two-dimensional scan was performed with the following ranges and steps: m_{H^\pm} from 43 to 95 GeV/c^2 with 1 GeV/c^2 steps, and $\text{Br}(\text{H}^+\rightarrow\tau^+\nu)$ from 0 to 1 with 0.05 steps.

Figure 2 shows the observed background confidence level CL_b as a function of m_{H^\pm} and $\text{Br}(\text{H}^+\rightarrow\tau^+\nu)$. The observed confidence level is everywhere within $\pm 2\sigma$ of the background prediction, except for three small regions, as shown in Figure 2. Such regions result from the combination of small excesses, as compared to the background expectation, observed by two or three experiments. The first two mass regions, around 43 and 55 GeV/c^2 , are due to a slight excess of data in the hadronic channel, while the third one, around 90 GeV/c^2 , arises from an excess of events in the mixed channel. Table 3 gives the combined CL_b together with the values from each experiment for these three domains (the values chosen for $\text{Br}(\text{H}^+\rightarrow\tau^+\nu)$ are given in the second column).

The combined results for the Type II 2HDM are summarised in Figure 3, which shows the expected median and observed mass limits, while the contribution of each of the three decay channels to the overall limit is presented in Figure 4. It is worth noting that:

- the purely leptonic channel alone excludes charged Higgs masses above the W mass, down

m_{H^\pm} (GeV/ c^2)	$\text{Br}(H^+ \rightarrow \tau^+ \nu)$	combined CL_b	ALEPH CL_b	DELPHI CL_b	L3 CL_b	OPAL CL_b
43.	0.0	0.998	(*)	0.99	(*)	0.96
55.	0.0	0.997	0.75	0.96	0.96	0.94
89.	0.35	0.988	0.98	0.63	0.88	0.80

Table 3: *Combined and individual CL_b values for the three mass points with a deviation from expectation larger than 2σ . All values, obtained with the statistical procedure of the overall combination, compare well to those published by the experiments. (*) ALEPH and L3 did not provide inputs for this mass.*

to $\text{Br}(H^+ \rightarrow \tau^+ \nu)$ around 0.45. In this channel, the mass of the Higgs boson cannot be reconstructed, due to the presence of two neutrinos in the final state. As a consequence, the W boson pair background is diluted and the analysis is sensitive up to $\sqrt{s}/2$. The limit drops rapidly for $\text{Br}(H^+ \rightarrow \tau^+ \nu)$ below 0.45, due to a rapid decrease of the signal rate in this final state;

- the mixed channel alone cannot exclude charged Higgs mass values up to the W mass, even when it contributes maximally, for $\text{Br}(H^+ \rightarrow \tau^+ \nu) = 0.5$. For this value, the observed limit is only slightly above 79 GeV/ c^2 , due to the large $e^+e^- \rightarrow W^+W^-$ background. This channel has the best coverage in terms of $\text{Br}(H^+ \rightarrow \tau^+ \nu)$, as shown in Figure 4;
- the hadronic channel is the most difficult one; for masses close to the W mass, the sensitivity is reduced due to the large $e^+e^- \rightarrow W^+W^-$ background. The sensitivity at higher masses is improved (a gain of 10 GeV/ c^2 on the expected limit), and the observed limit as well (note the excluded “island” at $\text{Br}(H^+ \rightarrow \tau^+ \nu)$ close to zero) with respect to the results of individual experiments;
- the difference between the expected and observed limit seen in Figure 3 for $\text{Br}(H^+ \rightarrow \tau^+ \nu)$ from 0.35 to 0.85 results from the excess of observed events already mentioned (see Figure 2) in the mixed channel above $m_{H^\pm} = 84$ GeV/ c^2 .

The combined 95% C.L. m_{H^\pm} lower limits are listed in Table 4 for $\text{Br}(H^+ \rightarrow \tau^+ \nu) = 0, 1$, together with the limit that is independent of the fermionic decay mode. Taking the lowest of the observed limits from Table 4, we quote a 95% C.L. lower bound of 80 GeV/ c^2 for the mass of the charged Higgs boson in type II 2HDM under the assumption of pure fermionic decays of the charged Higgs boson. Thus the hypothesis of a charged Higgs boson degenerate in mass with the W boson is not excluded at the 95% confidence level with LEP data. The limits around the W mass are very sensitive to the modelling of the W pairs background. Taking the uncertainties in the background modelling into account results in a downward shift of these limits by 600 and 500 MeV/ c^2 for $\text{Br}(H^+ \rightarrow \tau^+ \nu) = 0$ and 0.5, respectively.

Figure 5 shows the 95% C.L. upper bound on the $e^+e^- \rightarrow H^+H^-$ cross-section (with $\pm 1\sigma$ and $\pm 2\sigma$ bands) for four values of $\text{Br}(H^+ \rightarrow \tau^+ \nu)$, namely 1, 0.5, 0.2 (which corresponds to

	H [±] mass limit (95% C.L.) in GeV/c ²
Br(H ⁺ →τ ⁺ ν)=0	
Expected limit (median)	88
Observed limit	80.5 (*)
Br(H ⁺ →τ ⁺ ν)=1	
Expected limit (median)	93.5
Observed limit	94
Any Br(H ⁺ →τ ⁺ ν)	
Expected limit (median)	79.5
Observed limit	80

Table 4: *The combined 95% C.L. lower bounds on the mass of the charged Higgs boson, expected and observed, for fixed values of the branching ratio $Br(H^+ \rightarrow \tau^+ \nu)$ and for any $Br(H^+ \rightarrow \tau^+ \nu)$. All mass limits have been rounded down to the nearest half a GeV/c² to take into account the effect of neglecting the correlations between systematic uncertainties. (*) The interval from 83 to 88 GeV/c² is also excluded at the 95% C.L..*

the weakest limit) and 0. The thick black curve is the 2HDM tree-level prediction for that cross-section.

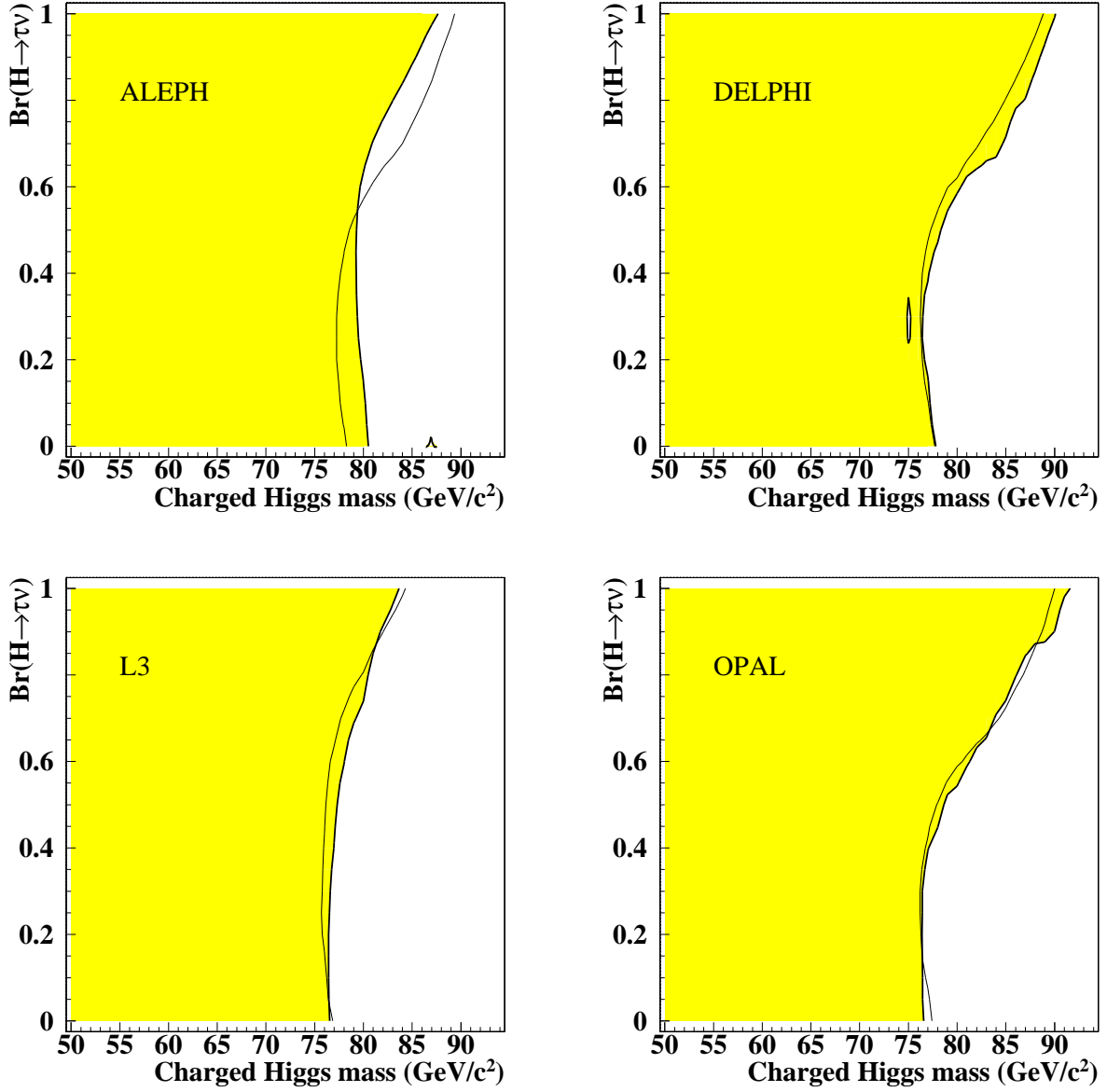


Figure 1: *Type II 2HDM: the 95% C.L. bounds on m_{H^\pm} as a function of the branching ratio $Br(H^+ \rightarrow \tau^+ \nu)$, for each of the four LEP experiments separately. The expected exclusion limits are indicated by the thin solid line and the observed limits by the thick solid line. The shaded area is excluded at the 95% C.L. or higher.*

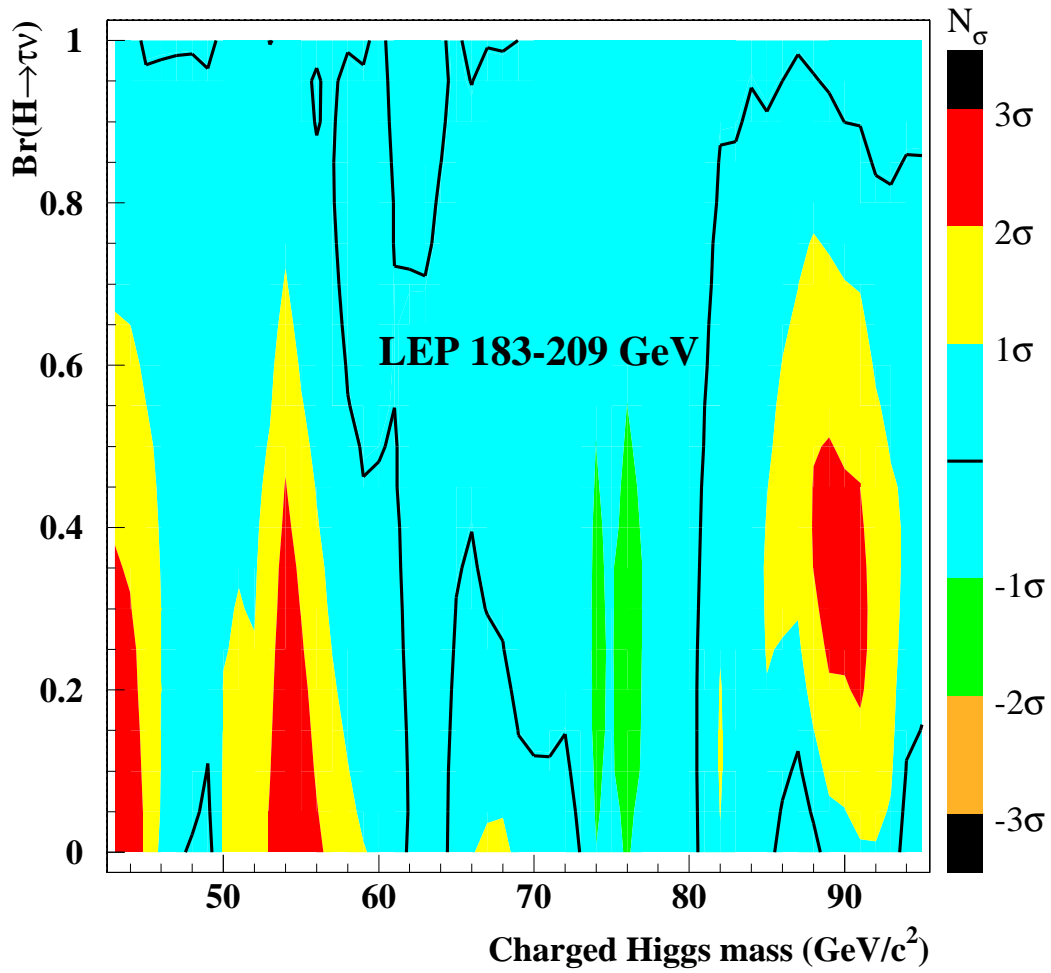


Figure 2: *Type II 2HDM: contours based on the observed p -values CL_b as a function of m_{H^\pm} and the branching ratio $\text{Br}(\text{H}^+ \rightarrow \tau^+ \nu)$, indicating the statistical significance, N_σ , of local departures from the background expectation. The black solid line indicates the change of sign of this significance, i.e. where there is a transition from excess to deficit.*

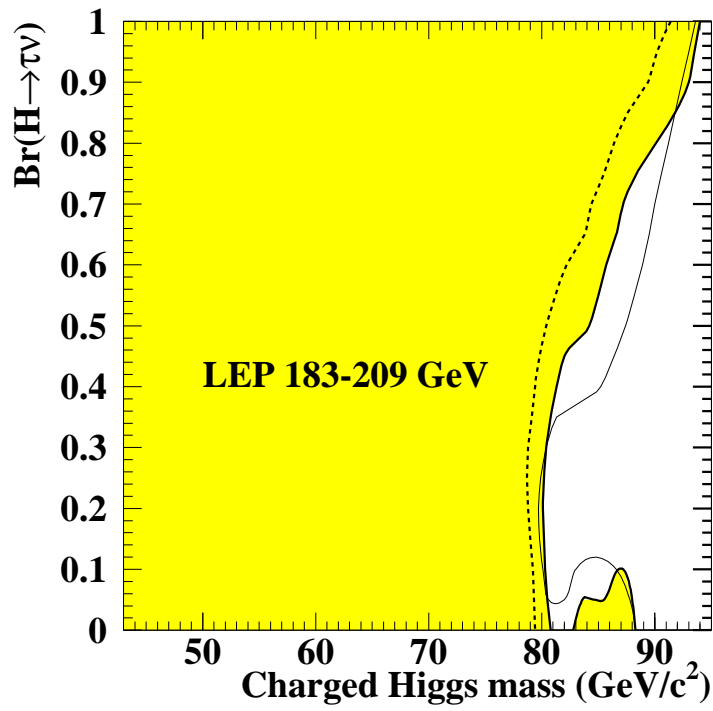


Figure 3: *Type II 2HDM: excluded regions in the $Br(H^+ \rightarrow \tau^+ \nu)$ vs m_{H^\pm} plane, based on the combined data collected by the four LEP experiments at centre-of-mass energies from 183 to 209 GeV. The shaded area is excluded at the 95% or higher C.L.. The expected exclusion limit (at the 95% C.L.) is indicated by the thin solid line and the thick dotted line inside the shaded area is the observed limit at the 99.7% C.L..*

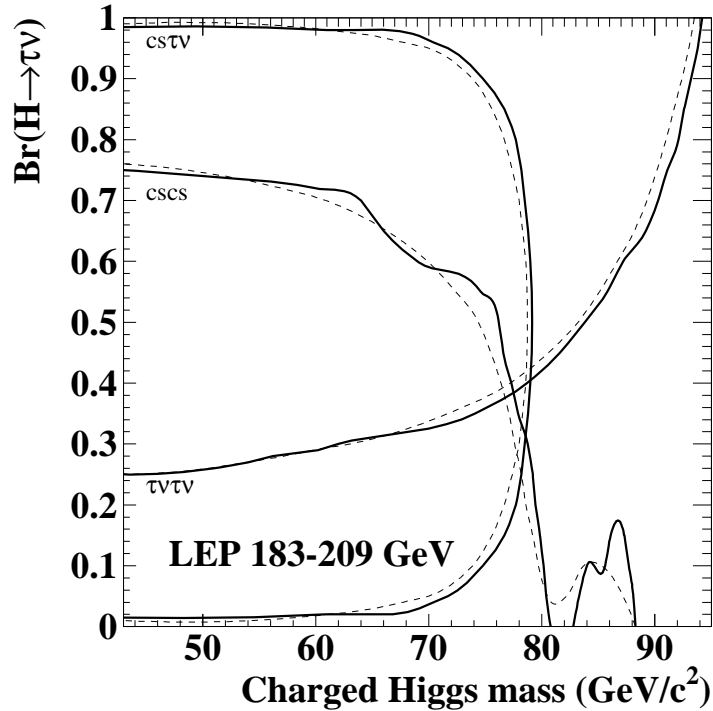


Figure 4: *Type II 2HDM: regions in the $Br(H^+ \rightarrow \tau^+ \nu)$ vs m_{H^\pm} plane excluded at the 95% or higher C.L., based on the combined data collected by the four LEP experiments at centre-of-mass energies from 183 to 209 GeV, for each of the three decay channels separately. The solid (dashed) lines are the observed (expected) limits.*

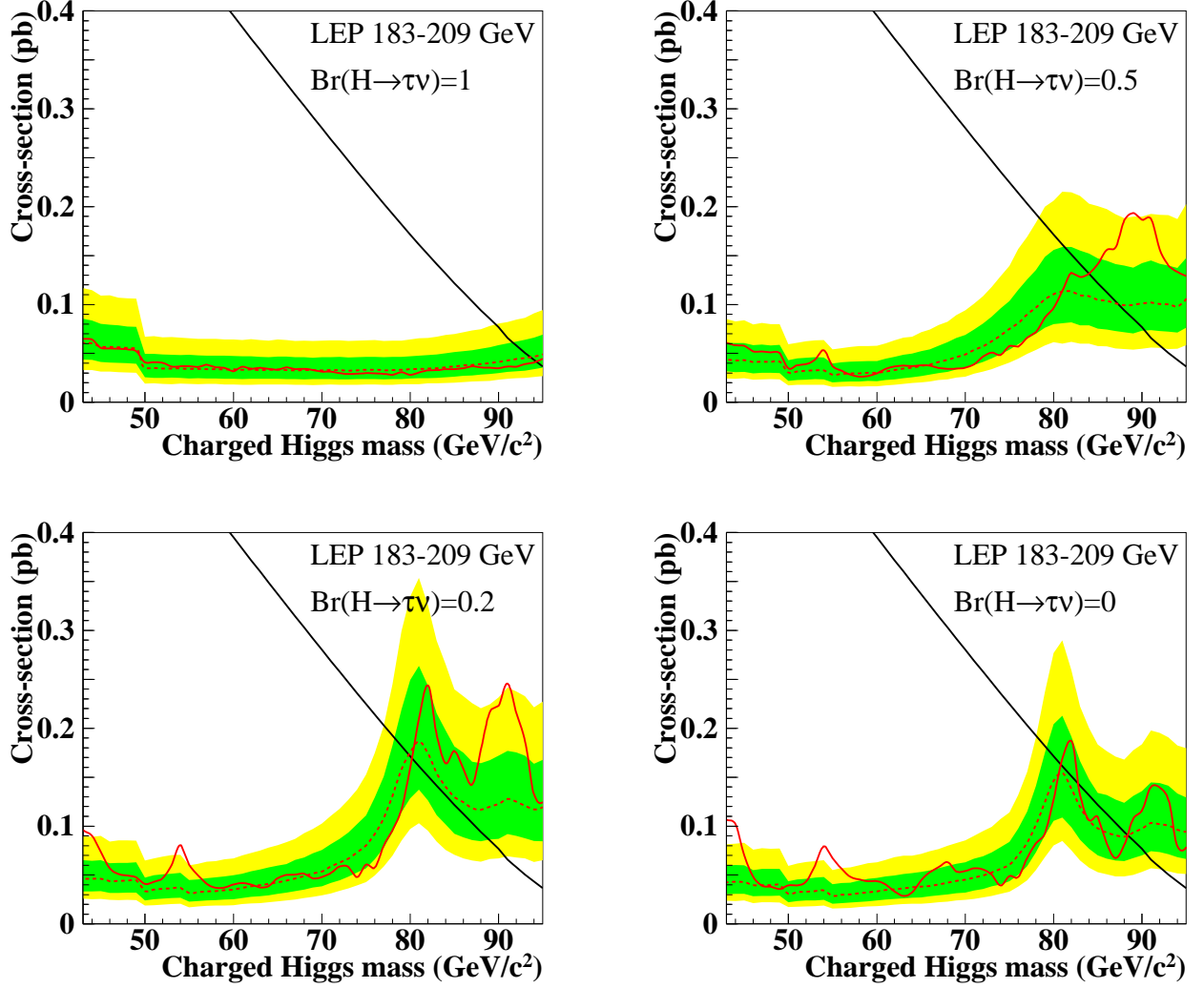


Figure 5: *Type II 2HDM: the 95% C.L. upper limits on the production cross-section as a function of m_{H^\pm} for four different values of the branching ratio $Br(H^+ \rightarrow \tau^+ \nu)$, combining the data collected by the four LEP experiments at centre-of-mass energies from 183 to 209 GeV. The solid lines represent the observed exclusion limits, while the expected exclusion limits are indicated by the dashed lines. The shaded bands represent the $\pm 1\sigma$ and $\pm 2\sigma$ excursions around the expected limits. The intersections of the curves (solid or dashed) with the thick line showing the theoretical (tree-level) charged Higgs cross-section represent the (observed or expected) 95% C.L. lower limits on the charged Higgs boson mass.*

3 Combined searches in 2HDM of type I

An alternative set of models, type I 2HDMs [10], assume that all fermions couple to the same Higgs doublet. In this case all fermions couple proportionately to $1/\tan\beta$ to the charged Higgs boson and fermionic decays are suppressed for medium to large $\tan\beta$ values. Consequently, if a neutral Higgs boson Φ (representing either A or the lightest CP-even scalar h) is sufficiently light, the decay to $W^*\Phi$ can be dominant even in the range of charged Higgs masses of interest at LEP (where W^* indicates an off-shell W boson). While searches for a CP-even neutral Higgs boson exclude such a particle for masses below $82 \text{ GeV}/c^2$ independently of its decay [27], the existence of a light CP-odd neutral Higgs boson, A, is not excluded by experiment [28]. Hence, the search for the process $H^\pm \rightarrow W^*A$ is fully justified. Figure 6 shows the predicted branching ratios of the charged Higgs bosons for various choices of parameters of type I models. For all kinematically allowed values of the A mass, m_A , the possible charged Higgs boson decays are predominantly fermionic for low $\tan\beta$ and predominantly bosonic for high $\tan\beta$. Between these two extreme cases, the branching ratios change rapidly as a function of $\tan\beta$ (between typically 0.1 and 10) and slower as a function of m_A , appearing earlier in $\tan\beta$ for lower m_A . The ratio between the two competing fermionic decays ($\tau\nu$ over $c\bar{s}$) is almost independent of the charged Higgs boson mass (see lower part of the figure), as expected from the Yukawa coupling which only depends upon the masses involved.

To cover the possibility of a light A boson the final states W^*AW^*A and $W^*A\tau^-\bar{\nu}_\tau$ were also searched for by DELPHI [3] and OPAL [6]. The channel $W^*A\bar{c}s$ was not considered because its contribution is expected to be small for all $\tan\beta$. The A boson was searched for through its decay into two b-jets, restricting the A mass to be above $12 \text{ GeV}/c^2$. Type I models are explored through the combination of all five decay channels, namely the final states $c\bar{s}c\bar{s}$, $c\bar{s}\tau\nu$, $\tau^+\nu\tau^-\bar{\nu}$, W^*AW^*A and $W^*A\tau^-\bar{\nu}_\tau$ (and their charge conjugates). The combination of the experimental search results is performed for branching ratio values predicted by the model as a function of $\tan\beta$ and m_A . Where there was a possible overlap between two search channels, the one providing less expected sensitivity was ignored to avoid double counting. This is the case in the intermediate region in $\tan\beta$ for purely hadronic channels (W^*AW^*A and $c\bar{s}c\bar{s}$) on the one hand and the semi-leptonic channels ($W^*A\tau^-\bar{\nu}_\tau$ and $c\bar{s}\tau^-\bar{\nu}$) on the other. A three-dimensional scan was performed with the following ranges and steps: m_{H^\pm} from 43 to 95 GeV/c^2 in 1 GeV/c^2 steps, m_A covering 12 GeV/c^2 , then 15 to 75 GeV/c^2 in 5 GeV/c^2 steps, and $\tan\beta$ from 0.1 to 100 in steps of 0.2 in $\log(\tan\beta)$.

Figure 7 shows the observed CL_b , for four values of m_A and two values of $\tan\beta$. A slight excess for low and intermediate A masses in the high $\tan\beta$ region where the bosonic decays dominate is observed, resulting in observed limits generally weaker than expected (see Figure 8). Three main features are visible in Figure 8, two plateaux and a valley between them:

- the first plateau, at low $\tan\beta$, corresponds to the case when the fermionic channels dominate. Both expected and observed limits are above $86 \text{ GeV}/c^2$;
- the valley is somewhat of an artefact. It is due to the conservative approach of considering only the most sensitive channel when two overlapping channels contribute. The difference

between expected and observed mass limits reaches $4.5 \text{ GeV}/c^2$ in the extreme case (when $\tan\beta = 1.6$ and $m_A = 12 \text{ GeV}/c^2$);

- the second plateau, at high $\tan\beta$, corresponds to the case when the bosonic channels dominate. The small excess seen in Figure 7 corresponds to a small difference between expected and observed charged Higgs mass limits, which is always less than $2.2 \text{ GeV}/c^2$.

Table 5 summarizes these results. For low $\tan\beta$ ($\tan\beta$ below 0.5) where the bosonic contribution is vanishingly small, the m_{H^\pm} lower limits (above $86 \text{ GeV}/c^2$) are almost independent of m_A . On the other hand, for high $\tan\beta$ (equal to or greater than 10) where the bosonic channels dominate, the sensitivity is maximal for intermediate A masses (m_A around $50 \text{ GeV}/c^2$). Outside the valley, the limit is always above $84 \text{ GeV}/c^2$. Finally, the lowest limits always correspond to the cases in the valley, thus depending both on $\tan\beta$ and m_A . The lowest (observed) limit is $72.5 \text{ GeV}/c^2$, for $\tan\beta = 1.6$ and $m_A = 12 \text{ GeV}/c^2$. This limit rises to $76.5 \text{ GeV}/c^2$ for $m_A = 20 \text{ GeV}/c^2$ and the difference between expectation and observation is reduced to $1 \text{ GeV}/c^2$.

m_A	$\tan\beta = 0.1$	$\tan\beta = 1$	$\tan\beta = 10$	$\tan\beta = 100$	minimum
12	86.0 (86.0)	73.5 (77.0)	83.5 (86.0)	84.0 (86.0)	72.5 (77.0)
20	86.5 (86.0)	76.5 (77.5)	85.5 (87.0)	85.5 (87.0)	76.5 (77.5)
30	86.5 (86.5)	80.0 (79.5)	87.5 (89.0)	87.5 (89.0)	78.0 (79.5)
50	86.5 (86.5)	84.0 (84.0)	89.0 (90.0)	89.5 (91.0)	81.0 (80.5)
70	86.5 (86.5)	86.5 (86.5)	83.5 (83.5)	89.0 (90.5)	81.0 (81.0)
minimum	86.0 (86.0)	73.5 (77.0)	81.5 (81.0)	81.0 (81.0)	72.5 (77.0)

Table 5: *Observed lower limits on the charged Higgs mass in GeV/c^2 at 95% C.L. for different values of m_A (in GeV/c^2) and $\tan\beta$. The expected median limits are shown in parentheses. The last column (last row) show the weakest limit for a fixed A mass and any $\tan\beta$ (for a fixed $\tan\beta$ and any A mass). The mass limits have been rounded down to the nearest half a GeV/c^2 to take into account the effect of neglecting correlations between systematic uncertainties.*

Figure 9 shows the excluded regions at the 95% C.L. in the plane $(m_{H^\pm}, \tan\beta)$ for four values of m_A , namely 12, 30, 50 and $70 \text{ GeV}/c^2$, together with the expected exclusion limits.

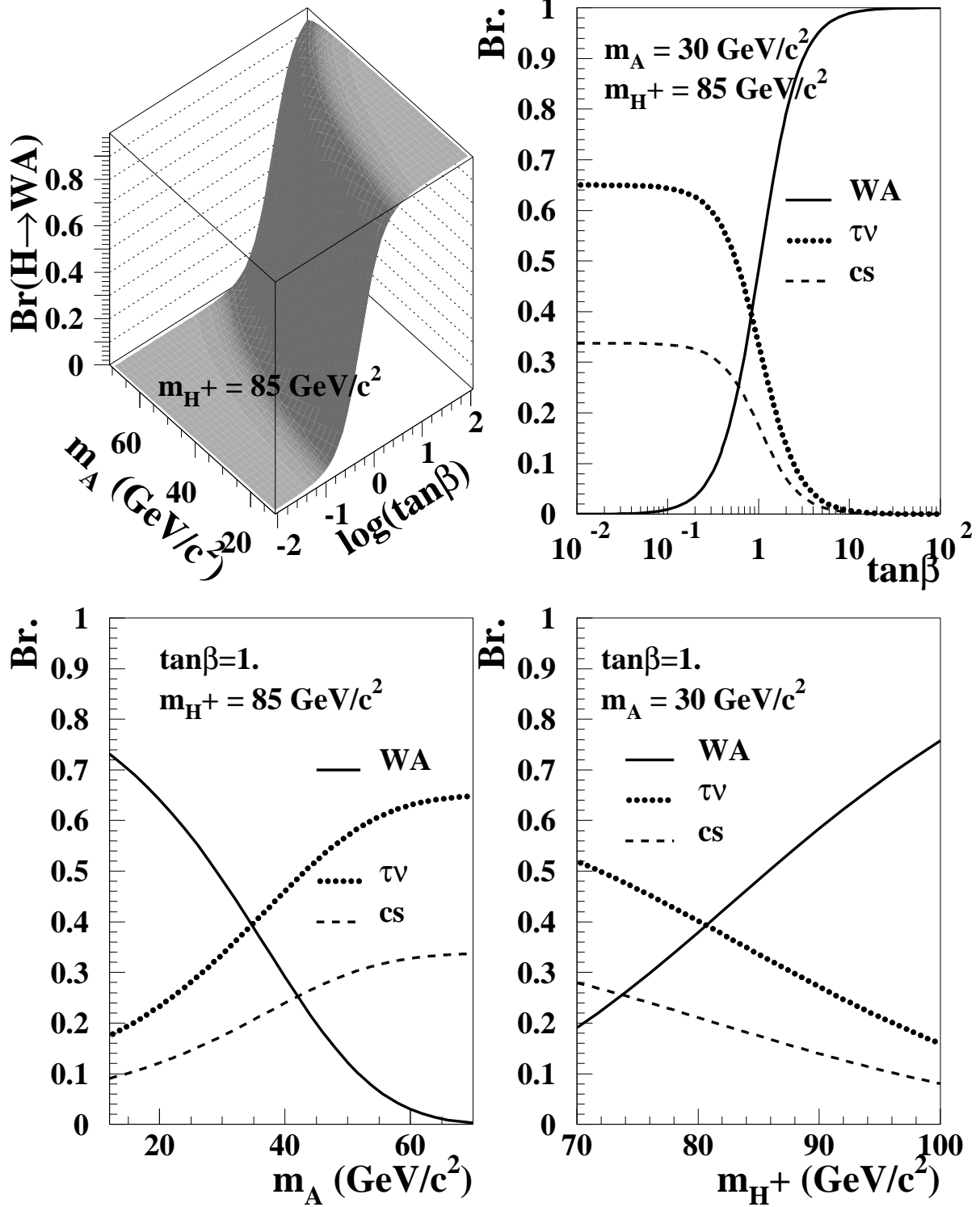


Figure 6: *Type I 2HDM: decay branching fractions as functions of the boson masses and $\tan\beta$.*

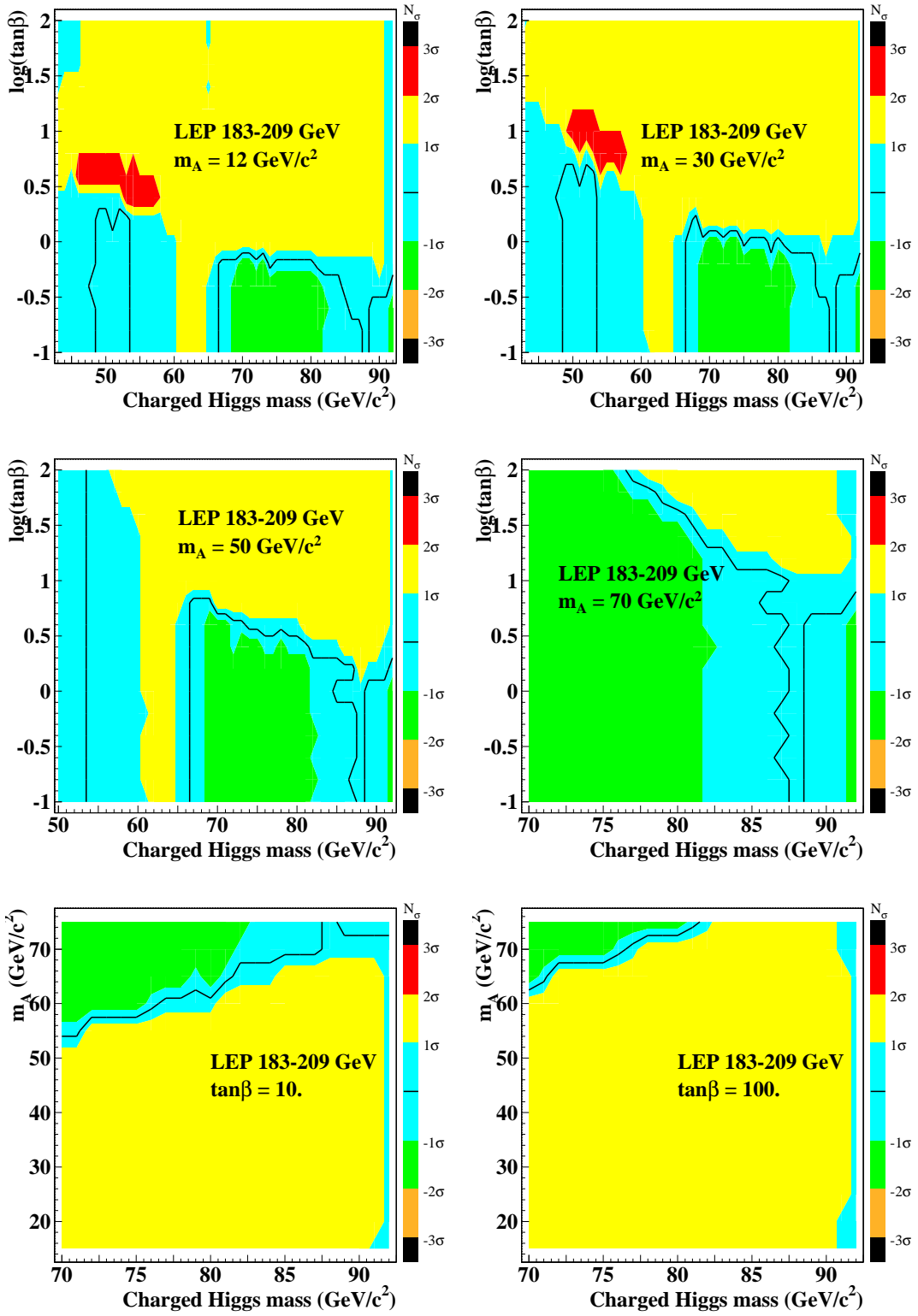


Figure 7: *Type I 2HDM: contours based on the observed p -values CL_b as a function of m_{H^\pm} and $\tan\beta$ or m_A , indicating the statistical significance, N_σ , of local departures from the background expectation, for four values of m_A and two values of $\tan\beta$. The black solid line indicates the change of sign of this significance, i.e. where there is a transition from excess to deficit.*

LEP 183-209 GeV

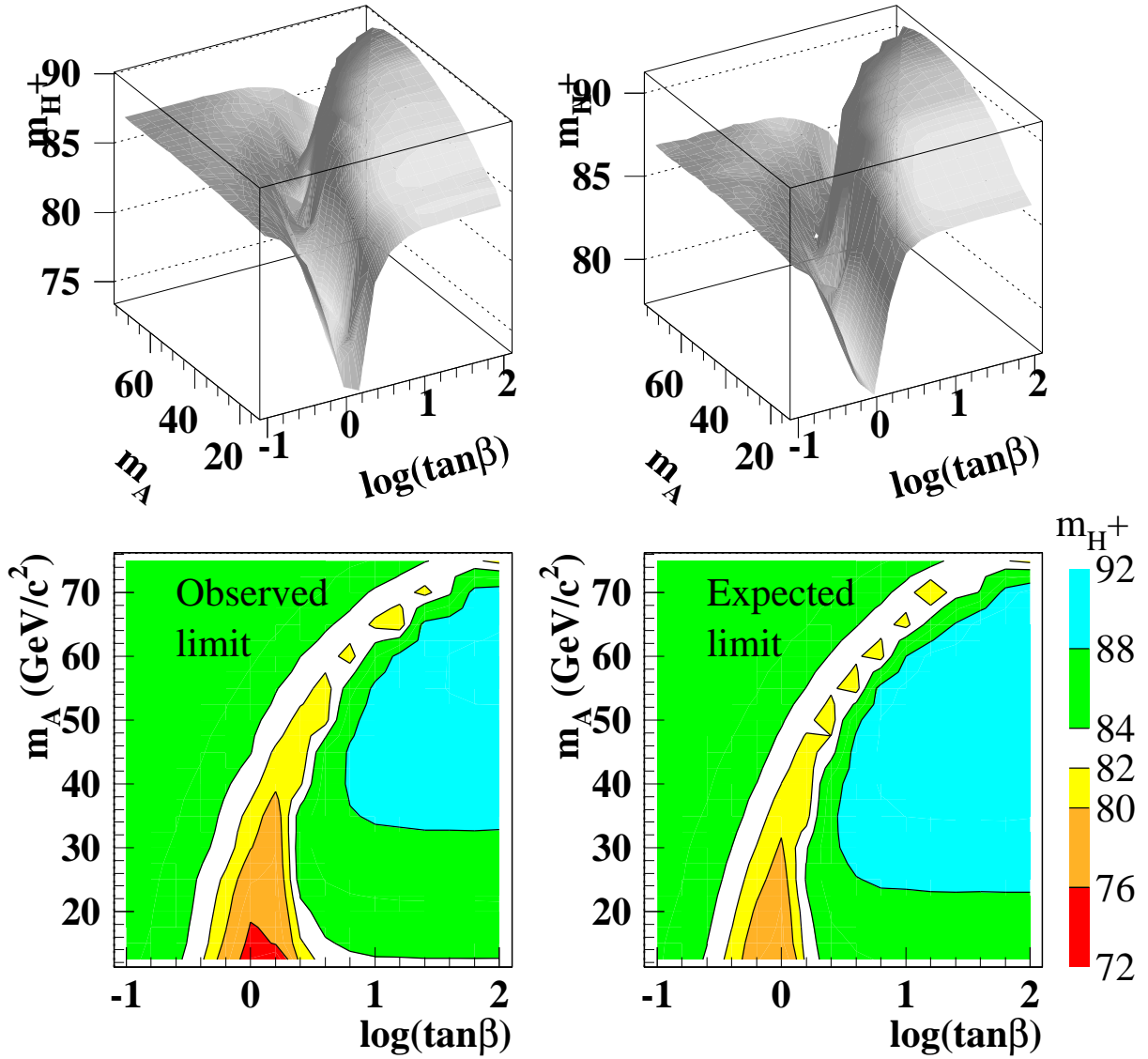


Figure 8: Type I 2HDM: Observed (left) and expected (right) 95% C.L. lower limits on the mass of the charged Higgs boson. The colour-mass correspondence is indicated on the right hand side (units are GeV/c²).

LEP 183-209 GeV

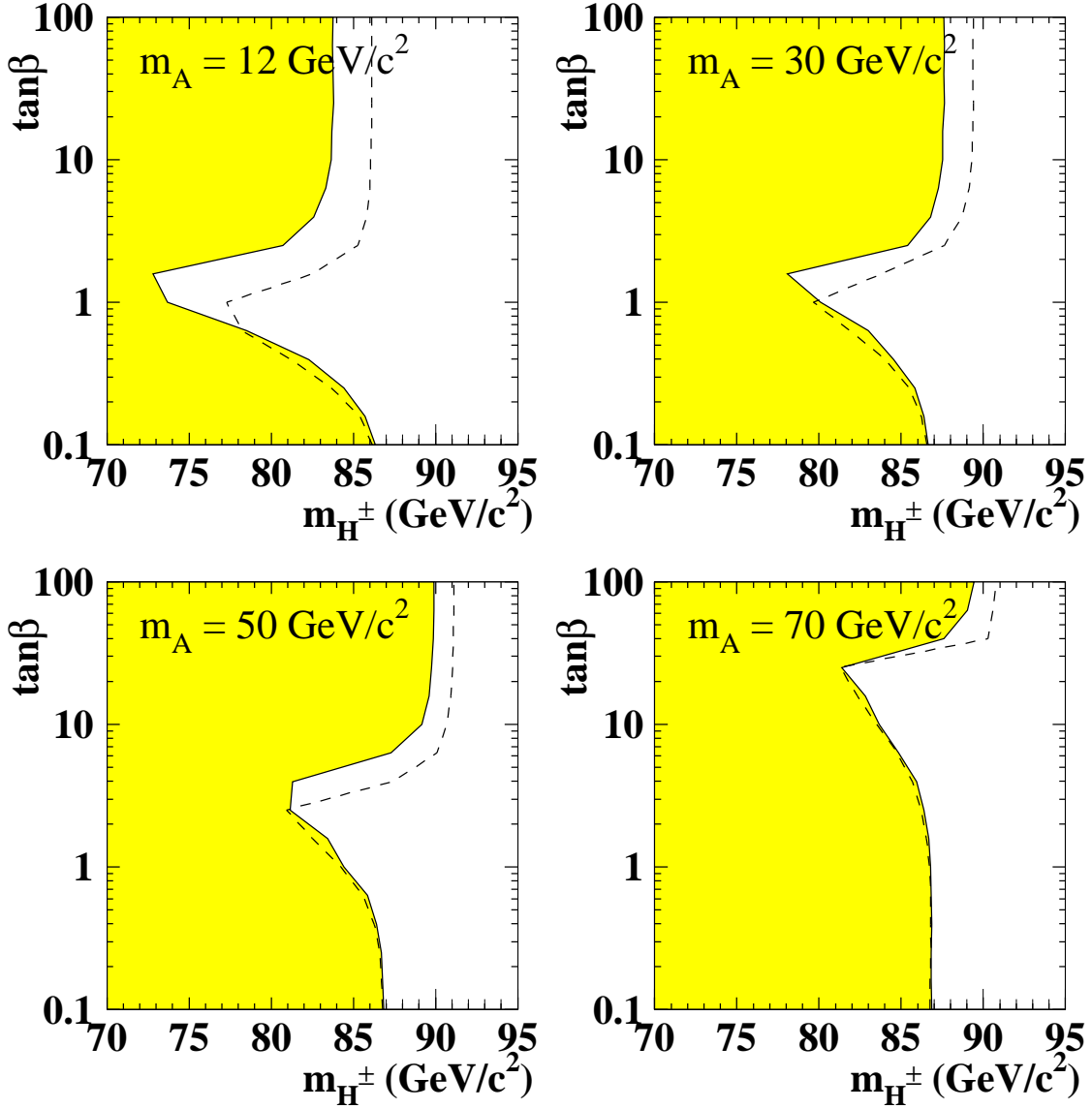


Figure 9: *Type I 2HDM: Excluded regions at 95% C.L. in the $(m_{H^\pm}, \tan\beta)$ plane for different values of m_A : 12, 30, 50 and 70 GeV/c². The dashed line represents the expected exclusion limit.*

4 Summary

The results of the searches carried out by the four LEP experiments for charged Higgs bosons predicted by 2HDMs are statistically combined. No significant excess over the SM background is observed, and the exclusion limits are extended by several GeV/c^2 with respect to the final results of the individual collaborations [2,3,5,6] and the previous combination [1]. In the type II 2HDM scenario, assuming that the two decays $H^+ \rightarrow c\bar{s}$ and $H^+ \rightarrow \tau^+\nu$ exhaust the H^+ decay width, mass limits are obtained as a function of the branching ratio $\text{Br}(H^+ \rightarrow \tau^+\nu)$. A 95% C.L. lower limit on the charged Higgs mass, independent of the boson decay mode, is found to be $80 \text{ GeV}/c^2$. A new scenario, for type I 2HDM, thanks to analyses by DELPHI and OPAL in the bosonic W^*A decay channels, is also performed. In this case, masses of the charged Higgs boson below $72.5 \text{ GeV}/c^2$ are excluded at the 95% C.L. for A masses above $12 \text{ GeV}/c^2$.

Acknowledgements

We would like to thank the CERN accelerator division for the excellent performance of the LEP accelerator in its high-energy phase. The LEP working group for Higgs boson searches would also like to thank the members of the four LEP experiments for providing their results and for valuable discussions concerning their combination.

References

- [1] Search for Charged Higgs bosons: preliminary combined results using LEP data collected at energies up to 209 GeV. LHWG Note/2001-05, July 2001, and hep-ex/0107031.
- [2] A. Heister *et al.* (ALEPH Collaboration), Phys. Lett. **B543** (2002) 1.
- [3] J. Abdallah *et al.* (DELPHI Collaboration), Eur. Phys. J. **C34** (2004) 399.
- [4] P. Abreu *et al.* (DELPHI Collaboration), Phys. Lett. **B460** (1999) 484.
- [5] P. Achard *et al.* (L3 Collaboration), Phys. Lett. **B575** (2003) 208.
- [6] G. Abbiendi *et al.* (OPAL Collaboration), Eur. Phys. J. **C72** (2012) 2076.
- [7] G. Abbiendi *et al.* (OPAL Collaboration), Eur. Phys. J. **C7** (1999) 407.
- [8] The LEP Working Group for Higgs Boson Searches consists of members of the four LEP collaborations and of theorists among whom S. Heinemeyer is co-author of this paper.
- [9] H.E. Haber *et al.*, Nucl. Phys. **B161** (1979) 493.

- [10] S.L. Glashow and S. Weinberg, Phys. Rev. **D15** (1977) 1958.
E.A. Paschos, Phys. Rev. **D15** (1977) 1966.
A.G. Akeroyd, Nucl. Phys. **B544** (1999) 557.
- [11] The LEP Collaborations, the SLD Collaboration, the LEP Electroweak working group, the SLD Electroweak and Heavy Flavour Groups, Phys. Rep. **427** (2006) 257.
- [12] D. Decamp *et al.* (ALEPH Collaboration), Phys. Rep. **216** (1992) 253.
- [13] P. Abreu *et al.* (DELPHI Collaboration), Z. Phys. **C64** (1994) 183.
- [14] O. Adriani *et al.* (L3 Collaboration), Z. Phys. **C57** (1993) 355.
- [15] G. Alexander *et al.* (OPAL Collaboration), Phys. Lett. **B370** (1996) 174.
- [16] The HZHA Generator: G. Ganis and P. Janot, CERN Report 96-01, Vol. 2, p. 309 (1996);
Version 3, released in December 1999, <https://janot.web.cern.ch/janot/Generators.html>.
- [17] A.G. Akeroyd *et al.*, Eur. Phys. J. **C12** (2000) 451.
- [18] M. Skrzypek *et al.*, Comp. Phys. Comm. **94** (1996) 216.
- [19] A. Denner *et al.*, Phys. Lett. **B475** (2000) 127.
- [20] S. Jadach *et al.*, Phys. Rev. **D61** (2000) 113010.
- [21] A. Ballestrero *et al.*, Comp. Phys. Comm. **152** (2003) 175.
- [22] J. Fujimoto *et al.*, Comp. Phys. Comm. **100** (1997) 128.
- [23] The LEP Collaborations, ALEPH, DELPHI, L3, OPAL, and the LEP Electroweak Working Group, Eprint arXiv:hep-ex/0612034 (2006).
- [24] ALEPH, DELPHI, L3 and OPAL Collaborations, The LEP working group for Higgs boson searches, Phys. Lett. **B565** (2003) 61.
- [25] R.D. Cousins and V.L. Highland, Nucl. Instr. Methods **A320** (1992) 331.
- [26] The LEP collaborations, The LEP working group for Higgs boson searches, Eur. Phys. J. **C47** (2006) 547.
- [27] G. Abbiendi *et al.* (OPAL Collaboration), Eur. Phys. J. **C27** (2003) 311.
- [28] J. Abdallah *et al.* (DELPHI Collaboration), Eur. Phys. J. **C38** (2004) 1.